JOURNAL OF AIRCRAFT
Vol. 32, No. 3, May–June 1995

Lift-Enhancing Tabs on Multielement Airfoils

James C. Ross*
NASA Ames Research Center, Moffett Field, California 94035-1000
Bruce L. Storms†
Sterling Software, Moffett Field, California 94035-1000
and
Paul G. Carrannanto‡
Ford Motor Company, Dearborn, Michigan 48121-2053

The use of flat-plate tabs (similar to Gurney flaps) to enhance the lift of multielement airfoils is extended here by placing them on the pressure side and near the trailing edge of the main element rather than just on the furthest downstream wing element. The tabs studied range in height from 0.125 to 1.25% of the airfoil reference chord. In practice, such tabs would be retracted when the high-lift system is stowed. The effectiveness of the concept was demonstrated experimentally and computationally on a two-dimensional NACA 63_2-215 Mod B airfoil with a single-slotted, 30%-chord flap. Both the experiments and computations showed that the tabs significantly increase the lift at a given angle of attack and the maximum lift coefficient of the airfoil. The computational results showed that the increased lift was a result of additional turning of the flow by the tab that reduced or eliminated flow separation on the flap. The best configuration tested, a 0.5%-chord tab placed 0.5% chord upstream of the trailing edge of the main element, increased the maximum lift coefficient of the airfoil by 12% and the maximum lift-to-drag ratio by 40%.

Nomenclature

C_d = section drag coefficient
C_l = section lift coefficient
C_p = pressure coefficient
c = airfoil chord
d = distance from tab to main-element trailing edge
g = flap gap, perpendicular to chordline
h = tab height
L/D = lift-to-drag ratio
ol = flap overlap
p = static pressure
q = dynamic pressure
Re = Reynolds number
V = velocity
δ = deflection angle

Subscripts
f = flap
max = maximum
∞ = freestream condition

Introduction

IN an increasingly competitive market for subsonic transport aircraft, the performance and complexity of the high-lift system have become more important in the design of new aircraft. Increased high-lift performance allows more flexibility in the cruise wing design whereas reduced system mechanical complexity lowers the manufacturing and operating costs of an airplane. The prospects for a large market for supersonic transport aircraft further increases the need for high-lift systems that have increased performance. For both types of aircraft, there is a requirement for reduced drag for takeoff configurations and increased maximum-lift and reduced angle of attack during landing. In order to satisfy these requirements, novel concepts should be explored. In this article, an experimental and theoretical study examining the lift capabilities of a two-element airfoil with Gurney-type flaps of various sizes placed at or near the trailing edge of the main element is described.

Liebeck[1] presented the first description of a Gurney flap. This flap consists of a small tab placed perpendicular to the pressure side at the trailing edge of the wing and is designed to produce a down-force on a racing car (Fig. 1). Although these flaps are generally less than 1% of the wing chord, they have a significant effect on the aerodynamic forces generated by the wing. Depending on the airfoil it is used on, the Gurney flap can increase the lift and decrease the drag while operating at high lift coefficients.

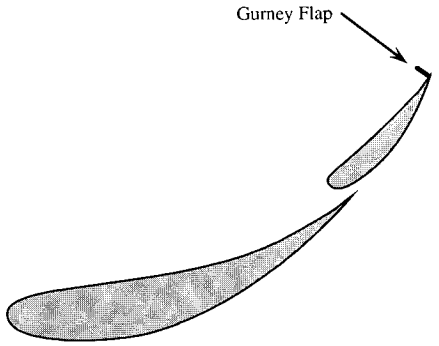

Fig. 1 Sketch of typical application of Gurney flap on a down-force-generating wing for racing cars.

Presented as Paper 93-3504 at the AIAA Applied Aerodynamics Conference, Monterey, CA, Aug. 9–11, 1993; received Oct. 2, 1993; revision received Oct. 15, 1994; accepted for publication Oct. 20, 1994.

*Aerospace Engineer, Fixed-Wing Aerodynamics Branch, NASA Ames Division. Senior Member AIAA.
†Aerospace Engineer. Member AIAA.
‡Product Design Engineer, Advanced Vehicle Systems Engineering. Member AIAA.

Several other researchers have studied this type of flap on single-element airfoils with similar results.[2–4] In general, as the flap height is increased, the maximum lift increases. For flap heights less than about 1.5% c, the maximum L/D can also increase. Flap heights greater than 1.5% c cause a decrease in the maximum L/D, but may still increase L/D at large lift coefficients. Computational and experimental results are given by Jang et al.[5] and Storms and Jang[6] for a single-element NACA 4412 airfoil. The results from Ref. 6 demonstrate the ability of a two-dimensional Navier–Stokes method to accurately compute the lift increase and, to a lesser extent, the drag increase resulting from various height Gurney flaps on the airfoil.

Katz and Largman[7] and Katz and Dykstra[8] showed the effect of a 5% c Gurney flap on the performance of multielement airfoils and wings for racing cars. These results showed that the flap increases the maximum aerodynamic lift, but the L/D is reduced relative to the airfoil or wing without the Gurney flap. The effect of smaller flaps was not discussed in these reports.

The design of aircraft high-lift systems differs from racing car wing design in that the multiple elements of the flap system must be stowed within the cruise-wing contour. This disrupts the camber at the trailing edges of airfoil elements containing cutouts for retracting other airfoil elements (coves). Proper shaping of the flaps and slats still results in good high-lift performance, but other means may be needed to increase performance for the next generation of aircraft. Deflecting the upper surface of the cover (or spoiler) on the main element has been proposed for transport aircraft[9] and is used on the F/A-18 fighter aircraft (Ref. 10 and Fig. 2). Results of spoiler droop on a transport aircraft airfoil showed a decrease in maximum lift for deflections of 5 and 10 deg, but an increase in the lift at a given angle of attack.[9]

Another approach to increasing lift is to place a tab on the trailing edge of airfoil elements that need additional aft camber. These tabs, which are less than 1% of the airfoil chord in height, are retracted when the high-lift system is stowed (Fig. 3). Since the tabs need not be located right at the trailing edge of the elements, installation of a hinge is simplified. In carrying high-lift system designs from small-scale development to implementation on a production aircraft, scale effects (e.g., Reynolds number, geometric fidelity, surface finish) can, in some instances, cause the system performance to be less than that measured in wind-tunnel tests.[9] The use of lift-enhancing tabs provides a simple means by which adjustments can be made in the effective gap between the main-element trailing edge and the flap. On a flap system that includes a tab, the adjustment consists of replacing the tab with one slightly larger or smaller. This kind of adjustment may recover some of the lost performance without the major expense of redesigning and fabricating new flap tracks and actuators that are needed to change the flap gap. Although this article discusses the use of tabs near the main-element trailing edge, tabs may also be used at the trailing edge of any airfoil element that could benefit from additional camber, including slats.

This article summarizes the two-dimensional results of a research program that examines the performance of the lift-enhancing tab concept for a two-element airfoil. The effect of tab size and tab location relative to the main-element trailing edge was studied computationally and experimentally. The work was done on a two-element NACA 63_2-215 Mod B airfoil[11] with a 30% c single-slotted flap.

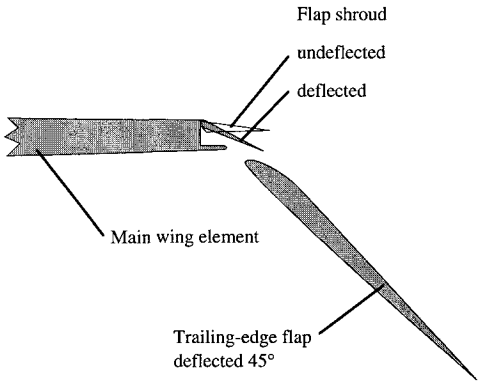

Fig. 2 Flap shroud used on F/A-18 aircraft in landing configuration. Similar to drooped spoiler from Ref. 9.

Experimental Setup

The airfoil geometry used in this study is shown in Fig. 4. The model was mounted between two false walls across the 7-ft dimension of the 7- × 10-ft wind tunnel no. 2 at NASA Ames Research Center (Fig. 5). A series of blowing slots was used to control the boundary layer in the junction between the model and the false walls. The model has a chord (flap stowed) of 2.5 ft and a span of 5.0 ft. Boundary-layer trip strips were located at 5 and 10% c on the upper and lower surfaces, respectively, of the main element. All of the data was obtained at a chord Reynolds number of 3.7×10^6. The freestream turbulence intensity in the 7- × 10-ft wind tunnel is 1% at the 225 ft/s test velocity.

The model was instrumented with 159 surface pressure taps arranged in three chordwise rows. The airfoil lift and pitching-moment coefficients were determined from pressure integrations along the row of taps on the model centerline. The other

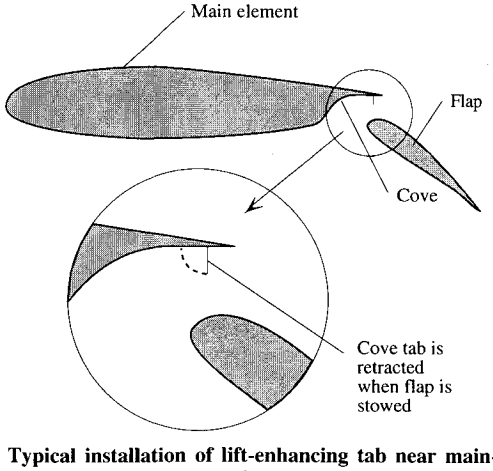

Fig. 3 Typical installation of lift-enhancing tab near main-element trailing edge of a two-element airfoil.

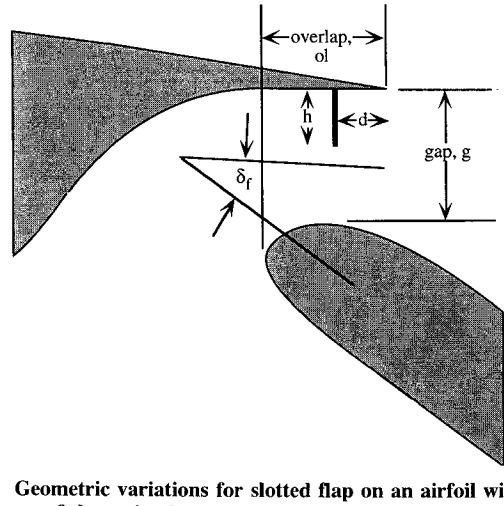

Fig. 4 Geometric variations for slotted flap on an airfoil with a tab in the cove of the main element.

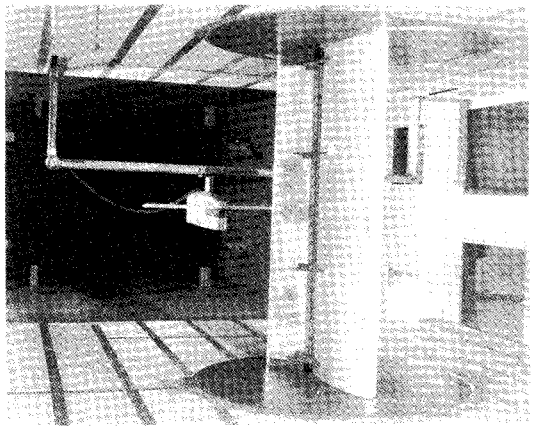

Fig. 5 NACA 63_2-215 Mod B airfoil model in 7- × 10-ft wind tunnel no. 2.

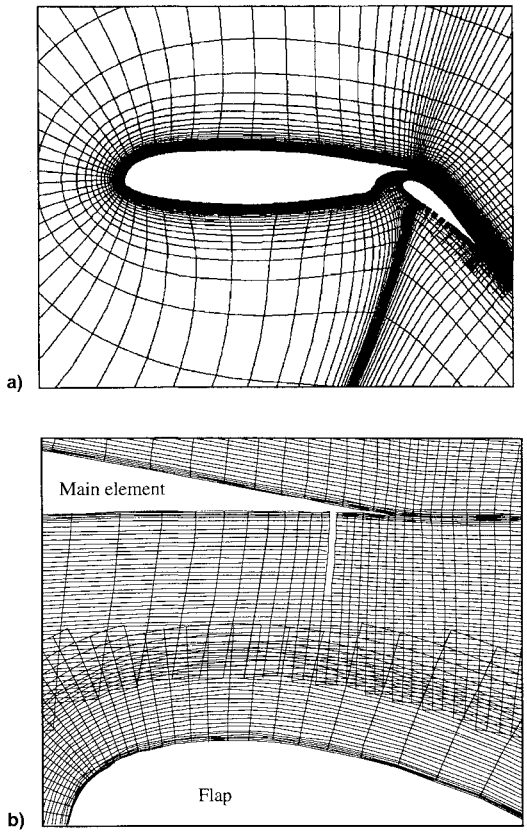

Fig. 6 Computational grid used in INS2D-UP; every other point omitted to improve clarity: a) overall grid and b) detail of grid at cove trailing edge to illustrate a tab in the grid.

two rows, located two-thirds of the way from the model centerline to each wall, were used to monitor the two dimensionality of the flow.

The drag was determined by integrating the total and static pressures measured using a rake located 0.7 chord downstream of the airfoil trailing edge. The method attributed to Betz[12] was used to account for variations in the static pressure due to flow curvature that occurs near the trailing edge of high-lift airfoils. The rake contained 91 total and 9 static pressure probes along its 36 in. length. The probes were clustered near the center of the rake to improve the spatial resolution in the region of large velocity gradients. The experimental setup is described in greater detail in Ref. 13.

The repeatability for the lift coefficient measurements was ± 0.020 for $C_l \leq 0.9 \cdot C_{l\max}$ and ± 0.04 for $C_l > 0.9 \cdot C_{l\max}$. For the drag coefficient measurements, the repeatability was ± 0.005 for $C_l \leq 0.9 \cdot C_{l\max}$, ± 0.010 for $0.9 \cdot C_{l\max} < C_l \leq C_{l\max}$, and ± 0.020 beyond $C_{l\max}$. These error bands include measurement resolution, point-to-point repeatability, and geometric uncertainties (i.e., slight variations in flap gap, overlap, and angle settings for repeat runs of a given geometry) and result in a maximum uncertainty of $\pm 5\%$ in the maximum L/D ratio measurements. The presence of flow separation on many of the configurations at large angles of attack adds an unknown bias error to the drag measurements. Given the repeatability of the measurements, differences between the various airfoil geometries can be discerned even if the absolute drag is not accurately known.

Two-Dimensional Computational Method

A concurrent computational study was performed to gain insight into the manner in which the tabs affect the flow around the airfoil. For the computations, the incompressible, Reynolds-averaged Navier–Stokes code INS2D-UP[14] employing the Baldwin–Barth turbulence model[15] was used. An earlier version of this code was used to compute the effect of various Gurney flaps on a single-element airfoil.[5,6] The code has also been shown to accurately compute the flow over multielement airfoils.[16]

The chimera[17] overset grid approach was used to develop computational grids around the two-element airfoil. Structured, hyperbolic grids were generated for each airfoil element using the HYPGEN code.[18] Points in each grid that lie inside the other airfoil element are removed from the com-

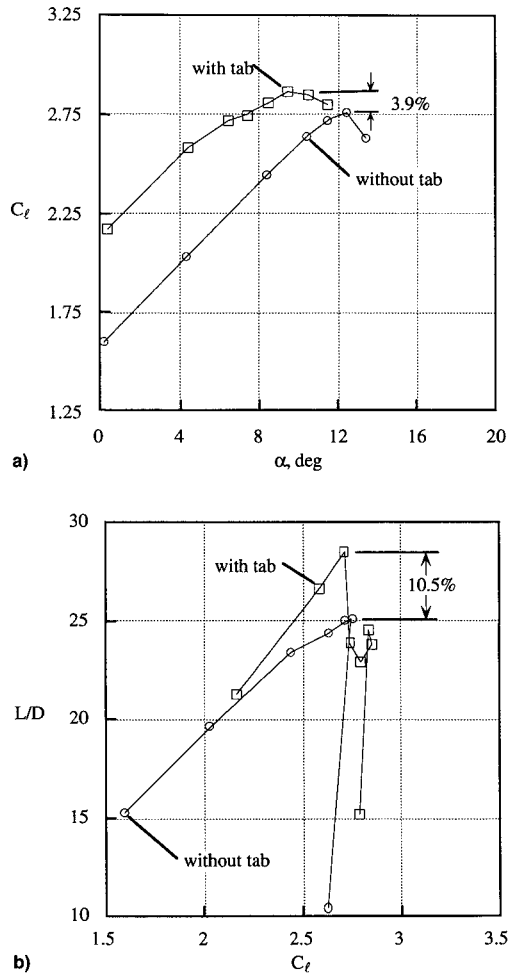

Fig. 7 Measured effect of 1% c tab located 1% c upstream of trailing edge of cove on two-element airfoil; NACA 63_2-215 Mod B, δ_f = 43.5 deg, g/c = 0.031, o/c = 0.042, Re = 3.7 × 10^6: a) lift coefficient vs angle of attack and b) L/D vs lift coefficient.

putation and the information is passed between the grids using interpolations generated by the code PEGSUS.[19] The grid is shown in Fig. 6a. Tabs are easily added to the computation by imposing no-slip boundary conditions on grid points that lie at the desired tab position (Fig. 6b). A complete description of the computational study is presented in Ref. 20.

Results

The flap geometry chosen for this study is a 43.5-deg flap deflection with a 3.1% c gap and 4.2% c overlap. An analysis of unpublished data acquired at NASA Ames Research Center shows that this geometry produces approximately 1.5% lower maximum section lift coefficient $C_{l\max}$ than did the best geometry. This flap rigging, without a tab on the main element, is used as the baseline for the following discussion.

The effect of a 1% c tab located 1% c upstream of the main-element trailing edge on the lift and drag of the airfoil is shown in Figs. 7a and 7b. The tab shifts the lift curve by approximately 5 deg at low angles of attack and increases the maximum lift coefficient by 3.9% (Fig. 7a). The tab also increases the maximum L/D of the airfoil by 29% (Fig. 7b). The tab increased the performance of the nonoptimized flap rigging above that of the optimized rigging for this airfoil.

Similar trends are shown in the computed lift and drag. The computations show a 5.3 deg shift in the lift curve and a 5.2% increase in maximum lift (Fig. 8a). The computed maximum L/D is increased by 8.8% when the 1% c tab is added (Fig. 8b). The primary difference between the computations and the experiment is that the computations indicate stall at a higher angle of attack than shown experimentally. While not exactly matching the measured lift and drag, the computations do indicate the proper trends for the changes in the aerodynamic forces when the tabs are added to the geometry. This is important if the computations are to be used to study the flows induced by the tabs.

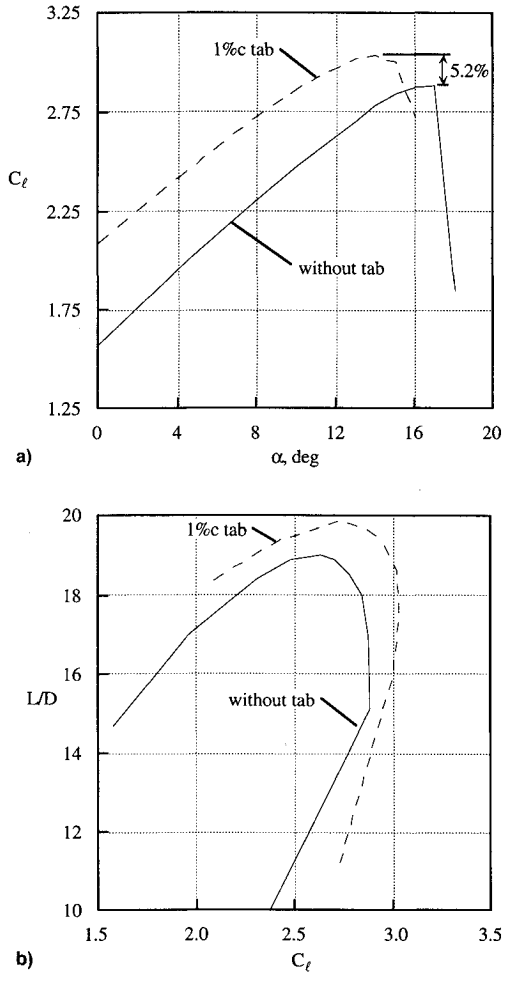

Fig. 8 Computed effect of 1% c tab located 1% c upstream of trailing edge of cove on two-element airfoil; NACA 63_2-215 Mod B, δ_f = 43.5 deg, g/c = 0.031, ol/c = 0.042, Re = 3.7 × 10^6: a) lift coefficient vs angle of attack and b) L/D vs lift coefficient.

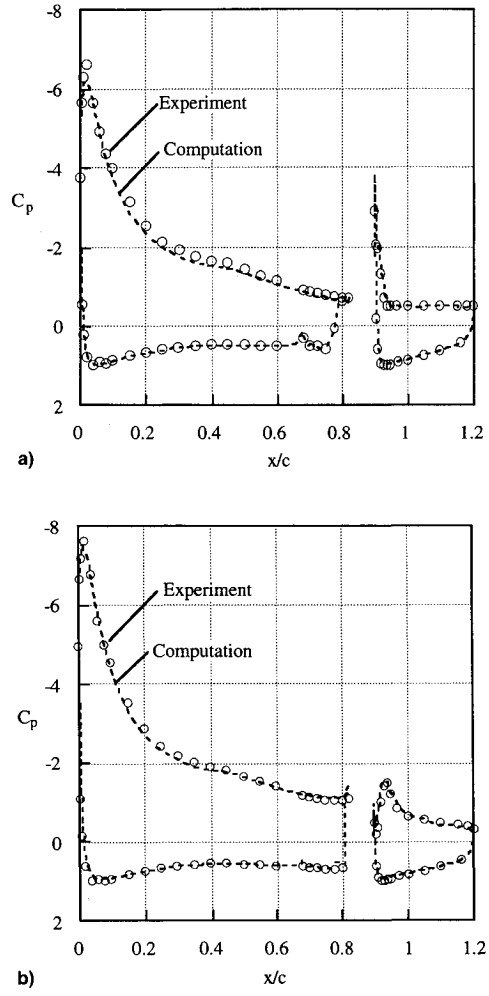

Fig. 9 Comparison of computed and measured pressure distributions for NACA 63_2-215 Mod B airfoil; α = 8.5 deg, δ_f = 43.5 deg, g/c = 0.031, ol/c = 0.042, Re = 3.7 × 10^6: a) no tab in main-element cove and b) 1% c tab located 1% c from main-element trailing edge.

Computed and measured pressure distributions are presented in Figs. 9a and 9b for the airfoil at an 8.5-deg angle of attack. The baseline results are shown in Fig. 9a and indicate that the flow over the flap separates at approximately 10% of the flap chord. The computed pressures are in good agreement with the measured values except for a slight underprediction of the suction on the main-element upper surface.

The same comparison of pressure distributions is shown in Fig. 9b for the configuration with a 1% c tab located 1% c from the main-element trailing edge. The effect of the tab is to increase the loading on the main element and to reattach the flow on the flap. Flow over the flap is able to remain attached with the tab because of the suppression of the large suction peak at the flap leading edge (sometimes referred to as a downwash effect). As a result, the flap normal force is increased slightly. The loading on the main element is increased significantly, particularly near the trailing edge. The pressure at the upper-surface trailing edge is reduced by the tab, which lowers the pressure gradient experienced by the boundary layer for a given lift coefficient.

The effect of the tab on the pressure distribution is different from that caused by simply deflecting the main-element trailing edge. Figure 10 illustrates the differences in the shapes of the pressure distributions near the main-element trailing edge for a deflected shroud and for a tab. If the effective angle of the flow leaving the trailing edge is the same for both geometries, the flap pressure distributions will not significantly differ for the two cases if the gap and overlap are maintained. The drooped-shroud case has a suction peak at the hinge point that limits the amount of deflection that can be used because of the large gradients downstream of the hinge. The pressure distribution for the tab case is much smoother and much less likely to cause premature flow separation than in the drooped-spoiler case.

The effect on the flow of a 1% c tab located 1% c forward of the main-element trailing edge is illustrated in Figs. 11a and 11b. Figure 11a shows computed streamlines for the airfoil without the tab. The flow exits smoothly from the main element at approximately the trailing-edge bisection angle and the flow separates from the flap at approximately 10% of the flap chord. In contrast, when the tab is in place, the flow exits from the main element in a direction approximately 20 deg downward from the bisector. By directing the flow downward as it leaves the main-element trailing edge, the tab reduces the loading on the flap, which allows the flow to remain attached on the flap upper surface. The tab also causes the main element to generate significantly more lift (Figs. 9a and 9b). A small recirculation region is located immediately downstream of the tab and a large, off-surface separation is located above the 60% c point on the flap. The off-surface separation results from the inability of the wake from the main element to sustain the adverse pressure gradient along its path above the flap.[16]

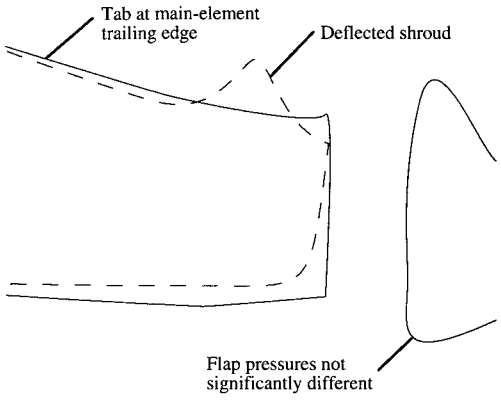

Fig. 10 Qualitative differences in pressure distributions for drooped shroud/spoiler[9] and cove tab.

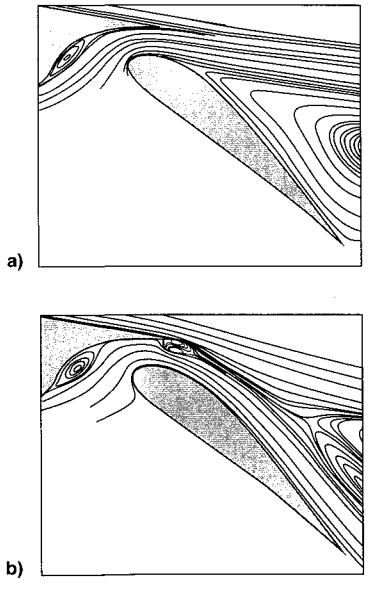

Fig. 11 Comparison of computed streamlines for baseline airfoil and airfoil with tab in cove; NACA 63_2-215 Mod B airfoil, Re = 3.7 × 10^6, α = 13 deg, δ_f = 43.5 deg, h/c = 0.005, d/c = 0.005: a) baseline airfoil and b) airfoil with 1% c tab 1% c upstream of trailing edge.

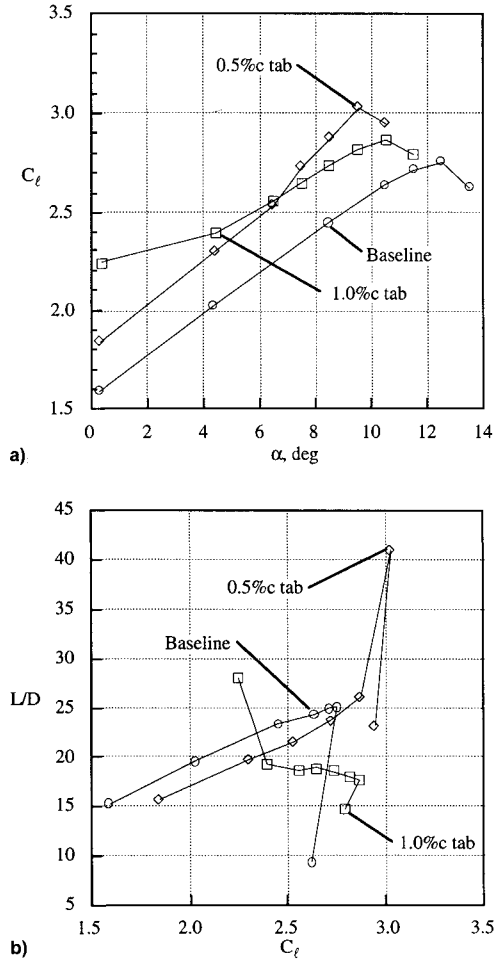

Fig. 12 Measured effect of tab height on airfoil performance with tabs at main-element trailing edge; NACA 63_2-215 Mod B, δ_f = 43.5 deg, g/c = 0.031, ol/c = 0.042, Re = 3.7 × 10^6: a) lift vs angle of attack and b) L/D vs lift coefficient.

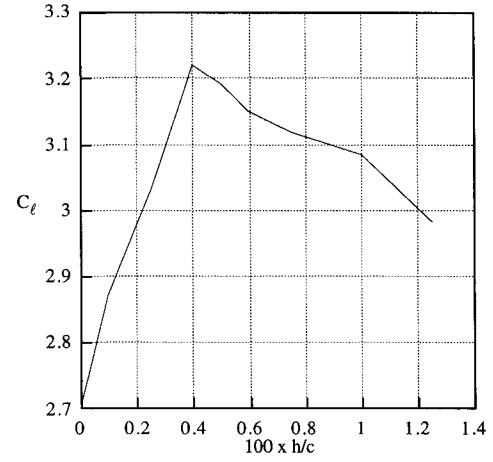

Fig. 13 Computed effect of tab height on airfoil lift coefficient with tabs at main-element trailing edge; NACA 63_2-215 Mod B, α = 13 deg, δ_f = 43.5 deg, g/c = 0.031, ol/c = 0.042, Re = 3.7 × 10^6.

A limited view of the effect of tab height on the lift of the airfoil is shown in Figs. 12a and 12b. The lift curve for the baseline configuration is plotted along with those for the 0.5% c and 1.0% c tabs located at the main-element trailing edge. The addition of the 0.5% c tab increased $C_{l\max}$ by approximately 9%, whereas a tab height of 1% c only increased $C_{l\max}$ by 3.5% (Fig. 12a). The abrupt increase in the slope of the lift curves for the tab configurations is due to the flow on the flap reattaching as the main element loading is increased. The baseline configuration, on the other hand, displayed separated flow on the flap throughout the angle-of-attack range. L/D was also affected by the tabs. Figure 12b shows that the addition of the 0.5% c tab increased the drag at a given lift coefficient for $C_l \leq 2.75$. At higher lift coefficients the drag was reduced, particularly just before $C_{l\max}$, at which point there was a dramatic reduction in drag. Again, this was due to the greatly improved flow on the flap. The 1% c tab had a larger effect on the drag, causing increased drag except at the lowest lift coefficient.

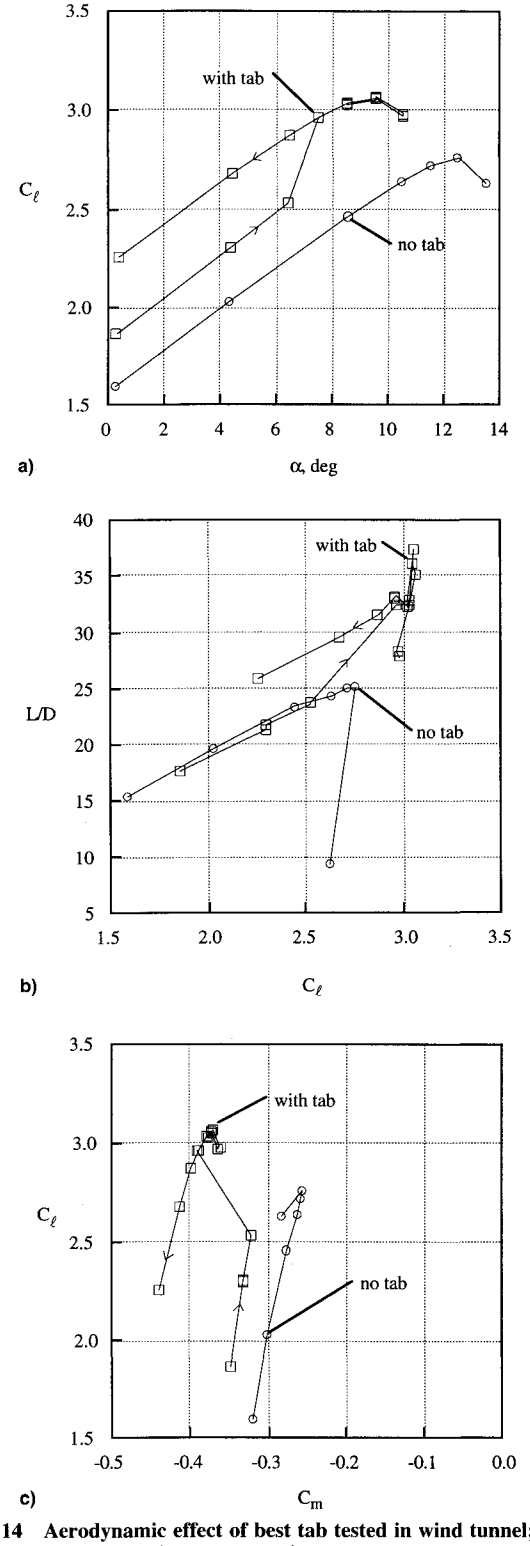

Fig. 14 Aerodynamic effect of best tab tested in wind tunnel; h/c = 0.005, d/c = 0.005, g/c = 0.031, ol/c = 0.042, δ_f = 43.5 deg, Re = 3.7 × 10⁶: a) lift coefficient vs angle of attack, b) L/D vs lift coefficient, and c) effect on pitching moment.

The effect of tab height was further examined computationally. The lift coefficient vs tab height is shown in Fig. 13 for a 13-deg angle of attack. This angle is approximately the angle of attack for maximum lift. The optimal height of a tab at the trailing edge of the main element (for this flap rigging) is between 0.4 and 0.5% c.

In the experiments, the most effective tab configuration was a 0.5% c tab located 0.5% c from the main-element trailing edge. The lift curve for this geometry is shown in Fig. 14a. The maximum lift in this case is 12% greater than that of the baseline configuration, and the maximum L/D is 40% greater than the baseline (Fig. 14b). Hysteresis is again apparent in both the lift and drag when the tab was in place. At low angles of attack the flow over the flap is separated. As the angle of attack is increased, the downwash of the main element causes the flow to reattach, increasing the lift of the whole airfoil. Once the flow is reattached, it is very stable and does not separate even when the angle of attack is reduced again. Similar (though opposite direction) hysteresis loops are reported in Ref. 21.

The lift increase available from tabs in the cove of the main element comes at the expense of increased nose-down pitching moment. Hysteresis is also present in the pitching-moment data (Fig. 14c). In conditions where the flow on the flap remains attached, the tab increases the nose-down moment by 33% relative to the baseline configuration.

Conclusions

The use of lift-enhancing tabs, or Gurney flaps, is extended to the main element of a two-element airfoil. Lift-enhancing tabs serve to increase the aft camber of the main element and to delay separation on the flap. Two-dimensional experiments showed that a 0.5% c tab, placed 0.5% c upstream of the main-element trailing edge of a two-element airfoil with a single-slotted flap, increases the $C_{l\max}$ by 12%. The maximum section L/D is increased by 40% as well. A companion computational study showed that the primary effect of the tab, when placed in the main-element trailing-edge cove, was to turn the flow toward the flap, thus reducing the effective angle of attack of the flap. The additional turning increases the lift of the main element and eliminates the separated flow on the flap. The pressure on the upper surface at the trailing edge is reduced by the tab, which also reduces the pressure gradient experienced by the boundary layer at a given lift coefficient. As with other effective trailing-edge high-lift devices, the tab in the main element cove increases the nose-down pitching moment.

References

[1]Liebeck, R. H., "Design of Subsonic Airfoils for High Lift," *Journal of Aircraft*, Vol. 15, No. 9, 1978, pp. 547–561.

[2]Neuhart, D. H., and Pendergraft, O. C., Jr., "A Water Tunnel Study of Gurney Flaps," NASA TM-4071, Nov. 1988.

[3]Roesch, P., and Vuillet, A., "New Designs for Improved Aerodynamic Stability on Recent Aerospatiale Helicopters," *Vertica*, Vol. 6, No. 3, 1982, pp. 145–164.

[4]Gregg, R. D., Hoch, R. W., and Henne, P. A., "Application of Divergent Trailing-Edge Airfoil Technology to the Design of a Derivative Wing," Society of Automotive Engineers TP 892288, Sept. 1989.

[5]Jang, C. S., Ross, J. C., and Cummings, R. M., "Computational

Evaluation of an Airfoil with a Gurney Flap," AIAA Paper 92-2708, June 1992.

[6]Storms, B. L., and Jang, C. S., "Lift Enhancement of an Airfoil Using a Gurney Flap and Vortex Generators," *AIAA Journal*, Vol. 31, No. 3, 1994, pp. 542–547.

[7]Katz, J., and Largman, R., "Effect of 90 Degree Flap on the Aerodynamics of a Two-Element Airfoil," *Journal of Fluids Engineering*, Vol. 111, March 1989, pp. 93, 94.

[8]Katz, J., and Dykstra, L., "Study of an Open-Wheel Racing-Car's Rear-Wing Aerodynamics," Society of Automotive Engineers TP 890600, Feb. 1989.

[9]Valarezo, W. O., Dominik, C. J., McGhee, R. J., and Goodman, W. L., "High Reynolds Number Configuration Development of a High-Lift Airfoil," AGARD Fluid Dynamics Panel Symposium High-Lift System Aerodynamics, Banff, Alberta, Canada, Oct. 1992.

[10]Meyn, L. A., Zell, P. T., Hagan, J. L., and Schoch, D., "Full-Scale Wind-Tunnel Tests of High-Lift System Modifications on a Carrier-Based Fighter Aircraft," AIAA Paper 93-1015, Feb. 1993.

[11]Hicks, R. M., and Schairer, E. T., "Effects of Upper Surface Modification on the Aerodynamic Characteristics of the NACA 63_2-215 Airfoil Section," NASA TM-78503, Feb. 1979.

[12]Schlichting, H., *Boundary-Layer Theory*, 7th ed., McGraw–Hill, San Francisco, CA, 1979, pp. 759–761.

[13]Storms, B. L., and Ross, J. C., "An Experimental Study of Lift-Enhancing Tabs on a Two-Element Airfoil," AIAA Paper 94-1868, June 1994.

[14]Rogers, S. E., Kwak, D., and Kiris, C., "Numerical Solution of the Incompressible Navier-Stokes Equation for Steady-State and Time-Dependent Problems," *AIAA Journal*, Vol. 29, No. 4, 1991, pp. 603–610.

[15]Baldwin, B., and Barth, T., "A One-Equation Turbulence Transport Model for High Reynolds Number Wall-Bounded Flows," AIAA Paper 91-0610, Jan. 1991.

[16]Rogers, S. E., "Progress in High-Lift Aerodynamic Calculations," AIAA Paper 93-0194, Jan. 1993.

[17]Benek, J. A., Buning, P. G., and Steger, J. L., "A 3-D Chimera Grid Embedding Technique," AIAA Paper 85-1523, July 1985.

[18]Chan, W. M., and Steger, J. L., "A Generalized Scheme for Three-Dimensional Hyperbolic Grid Generation," AIAA Paper 91-1586, June 1991.

[19]Tramel, T. W., and Suhs, N. E., "PEGSUS 4.0 User's Manual," Arnold Engineering Development Center TR-91-8, June 1991.

[20]Carrannanto, P. G., "Navier-Stokes Analysis of Lift Enhancing Tabs on Multi-Element Airfoils," M.S. Thesis, California Polytechnic State Univ., San Luis Obispo, CA, Aug. 1993.

[21]Biber, K., and Zumwalt, G. W., "Hysteresis Effects on Wind Tunnel Measurements of a Two-Element Airfoil," *AIAA Journal*, Vol. 31, No. 2, 1993, pp. 326–330.